Structural Integrity Evaluation of Fuel Test Loop Submerged in Water Subjected to Postulated Pipe Rupture

Choon-Yeol Lee*, Jae-Do Kwon, Yong-Son Lee
Department of Mechanical Engineering, Yeungnam University
Kil-Soo Kim
Korea Institute of Nuclear Safety
Jun-Yeun Kim
Korea Atomic Energy Research Institute

The structural integrity of the fuel test loop(FTL) in a Korean experimental reactor is evaluated when the FTL, submerged in a water environment, is subjected to a postulated pipe rupture. The analyses are performed under static and dynamic conditions, imposing the thrust force history at each postulated pipe rupture section. Through analysis the following results are found: 1) A double ended guillotine can not be expected based on the toughness of the material, 2) the structural integrity of the chimney surrounding the FTL would not impede the structural integrity by the pipe whip. All analyses are performed by finite element methods.

Key Words : Korean Experimental Reactor, Fuel Test Loop(FTL), Postulated Pipe Rupture, Structural Integrity, Seismic Analysis, Finite Element Method

1. Introduction

Nowadays, it is getting more important to evaluate reliability and to predict remaining life-time of the nuclear power plants. Numerous researches have been done on this subject through both of numerical and experimental methods including recent works by Kwon, Moon and Kim in 1998 and Song and Jhung in 1999. Especially, on nuclear piping systems, three different methods for prediction J-R curves were proposed and a computer program based on those J-R curve prediction methods was developed (Chang, Seok and Kim, 1997).

Recently, Battelle Northwest Research Institution evaluated the structural integrity of the fuel test loop(FTL) in the Korea multipurpose research reactor (KMRR) at Korea Atomic Research Institution (KAERI) (Battelle, 1995). In the evaluation, the effects of thrust force and jet impingement, which were caused by a postulated pipe rupture, on environments were investigated. The leak before break(LBB) concept was applied to the results and it was concluded that the dynamic analysis may not be required. However, KAERI recognized that the leakage detection of 1GPM(gallon per minute) to 10GPM is practically impossible, which was assumed in the report, since FTL is submerged in water and the pipe size, 63.5mm sch. 160, is too small to apply LBB concepts. The purpose of this paper is to give guidance for analyzing the effects of a loop rupture and pipe whip in a water environment. Hence, the present paper proposes a method to evaluate a structural integrity in water based on existing code and theory. In this paper, first, Battelle Research Institution's static model is regenerated and the results are compared. Secondly, from the results of the static analysis, the rupture section is determined based on ASME section Ⅲ. Thirdly, dynamic analyses are perfor-

* Corresponding Author,
E-mail : Cylee@ynucc. yu. ac. kr
TEL : +82-53-810-2570 ; **FAX** : +82-53-813-3703
Department of Mechanical Engineering, Yeungnam Univeristy, 214-1 Daedong, Kyungbuk, 712-749 Korea.
(Manuscript Received June 5, 1999; Revised October 11, 1999)

med on a ruptured pipe subjected to the prescribed thrust history in a water environment, since LBB concepts are not applicable. The calculations regarding thrust force history and jet impingement are performed using the results of ANSI/ANS-58. 2-1988.

2. Static and Seismic Analysis

2.1 Geometry and material property of pipe

FTL is made from austenitic stainless steel (301, 309, 319, 321 and 237) and covered with insulation material, whose material properties and geometric dimensions are listed in Table 1 and 2. Design pressure and temperature are 1.724kN/cm^2 and 328℃ respectively and saturation pressure is 1.25kN/cm^2.

2.2 Finite element analysis

The configuration of FTL and finite element node numbers are shown in Fig. 2.

As boundary conditions, node number 210, 120 and 10 representing pipe ends are fixed in all three directions. Node number 90 and 170, where support structures are located, are fixed in the x and y direction, respectively, while the z direction is free.

The static analysis is performed using ANSYS with dead weight of piping, internal pressure and thermal loading as loading conditions.

As a part of dynamic analysis, first, modal analysis is performed for seismic analysis. The analysis results show that the lowest and second modes are 6.0Hz and 7. 8Hz, respectively. The significant response in the first mode appears between nodes 210 and 170.

In order to perform the seismic analysis, used are the identical input ground acceleration spectrums with those of Battelle in the x, y and z

Table 1 Material properties of FTL

Young's modulus	17.256×10^6N/cm^2
Poisson's ratio	0.2642
Density	8.01×10^{-3}kg/cm^3
Thermal Expansion Coefficient	1.7790×10^{-5}/℃
Density of the Insulation	3.2989×10^{-3}kg/cm^3

Table 2 Geometric dimensions of FTL

Nominal Pipe Size	6.35cm. Sch. 160
Outside Diameter	7.3cm
Wall Thickness	0.953cm
Inside Diameter	5.398cm
Diameter of the Insulation	99.cm
Thickness of Insulation	0.127cm
Radius of Elbow	9.53cm
SIF at Elbow	0.9655

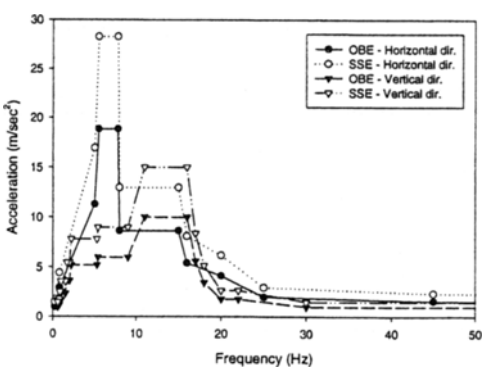

Fig. 1 Response spectrum for seismic analysis

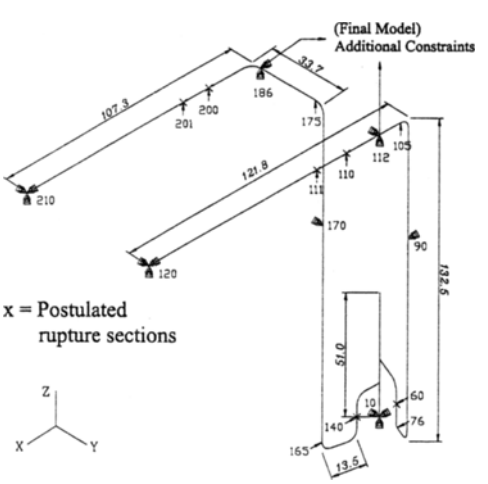

Fig. 2 The model for both static and dynamic analysis

direction, which are shown in Fig. 2. The maximum OBE ground acceleration in the x and y directions is 1.92g, and 1.02g in the z direction. The minimum value in the x, y and z directions is 0.1g. The imposed frequency range is 100Hz to 0. 6Hz. For SSE, the ground acceleration spectrum is given by 1.5 times the OBE ground acceleration spectrum. These spectrum are applied at the anchor locations, nodes 210, 120, 90, 170 and 10. Moreover, 2% damping was implied for the SSE horizontal and vertical reponse spectrum and 1% damping was used for OBE. The stress values at each element for each node are computed and the final stresses are calculated by SRSS (square root of square summation) method.

To calculate the maximum effective stress for various loading conditions, including static and seismic loadings for OBE and SSE, fifteen different kinds of combinations are considered: 1) Dead Weight (DW), 2) Internal Pressure (P), 3) Thermal Load (T), 4) DW+P, 5) DW+P+T, 6) DW+P+S_1+S_3 (Si: stress due to SSE in the i direction), 7) DW+P+S_2+S_3, 8~10) S_1, S_2 and S_3 for SSE, 11~15) similar stress combinations for OBE. The maximum effective stress is calculated and compared with that of Battelle and the present analysis, which justifies the present model and analysis as reasonable.

3. Dynamic Analysis of Postulated Rupture

3.1 Postulated rupture section

In general, the rupture sections are determined by using the criteria, class 2 of NUREG-0800 (standard review plan),

$$\sigma_a \leq 0.8\ (1.8S_h + S_a) \quad (1)$$

$$S_a = f(1.25S_c + 0.25S_h) \quad (2)$$

and the allowable effective stress σ_a is calculated to be 32.52kN/cm^2. From the maximum effective stress obtained through the various stress combinations mentioned above, all pipe section satisfy the condition and the postulated rupture sections can not be determined by using Eq. (1). Therefore, pipe rupture is postulated at the weakest sections, which correspond to the connecting sections of the pipes.

When a rupture occurs in the middle of the pipe, additional supports are needed to prevent the ruptured pipe section from rotating freely. Hence, for the analysis of ruptured pipe, nodes 112 and 186, where box beam supports are located, are fixed as in Fig. 2 in addition to the boundary conditions mentioned above.

3.2 Thrust force

Thrust force applied at the rupture section increases very rapidly at first when a rupture occurs. This initial thrust force will decrease according to the pressure drop in the pipe and it will reach a steady state. Eventually, the thrust force will be zero as pipe internal pressure drops to ambient pressure. The main response of the pipe is a transient response caused by the initial and steady thrust force. The initial and steady state thrust force and time required for steady state force can be found from ANSI/ANS-58.2-1988.

The initial thrust force, T_{int}, can be found from stagnation pressure and the cross sectional area of the pipe, which is calculated to be 39.4kN.

The steady state thrust force is a function of the friction in the pipe and stagnation enthalpy, which is 1.5×10^6J/kg at saturation pressure 1. 25kN/cm^2(328℃). The pressure loss, K_{tot}, can be found from the following expression,

$$K_{tot} = fL/D + K(90°\ el) + K(ent) \quad (3)$$

where f is friction factor depending on the pipe roughness and $K(90°\ el)$ and $K(ent)$ are equivalent pressure loss for 90° elbows and entrances, respectively. The total pipe length from in-pile system (IPS) to the break section, L, includes elbows at the ends, and is typically assumed to be 623.5cm. The total pressure loss is calculated to be 4.7. Using this value and Fig. B-7 in ANSI/ANS-58. 2-1988 at the stagnation enthalpy, the thrust coefficient, C_T, is found to be 0.62. Now, the steady state thrust force can be found:

$$T_s = C_T T_{int} = 24.4\ \text{kN} \quad (4)$$

The time required to steady state thrust can be found from

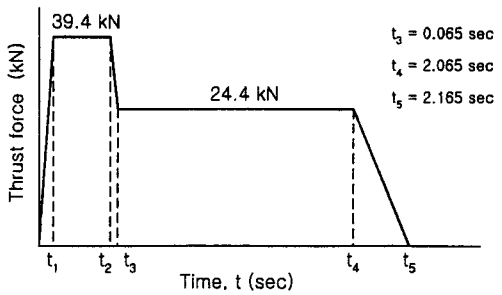

Fig. 3 Approximate force history applied at the broken sections

$$t_{ss}=(\rho_0/\rho_{sat})\,(c_o/u)\,(L/c_o) \tag{5}$$

where ρ_o/ρ_{sat} is the initial discharge density ratio and c_o/u is the ratio of sonic velocity to fluid velocity. From Eq. (5), the required time to reach the steady state thrust force is given to be 0.065sec. Now, a linearization between T_{int} and T_s is used and the thrust force history applied to the broken section is shown in Fig. 3.

3.3 Determination of damping

The FTL consists of thin steel pipe covered by insulation material and is surrounded by water. The damping in the air is assumed to be 2% (ζ, damping ratio) and the damping force is considered at 7.83Hz. Equivalent line density is found to be approximately 8.03×10^{-3}kg/cm^3 including steel pipe, insulation material, added mass and water inside the pipe. In order to obtain a smaller damping ratio for conservative analysis, the pipe is considered to be solid pipe with 9.9cm diameter corresponding to the outside diameter of the insulation. The mass, m of the pipe with 5.334m long solid pipe is calculated to be 347kg.

The damping factor in the air is obtained by assuming a single degree of freedom,

$$C=2\zeta m\omega_n=686\text{kg/sec} \tag{6}$$

The other damping factor is associated with damping of the fluid. The drag force is obtained from the equation,

$$F_D=C_D\left(\frac{\rho A|\bar{v}|}{2g}\right)V \tag{7}$$

where C_D: drag coefficient ($\sim$1.0), ρ: fluid density, 0.998×10^{-3}kg/cm^3(21.11℃), $\bar{v}$: initial velocity of the beam, A: projection area of the beam.

The damping coefficient associated with drag force is approximately

$$C_f=C_D\frac{\rho A|\bar{v}|}{2g} \tag{8}$$

The damping factor C_f is obtained if the initial velocity of the beam is known. The initial beam velocity is found from the energy conservation law. If 39.4kN is applied statically to the free end with l=5.334m, from the conservation of the strain energy and the work done in the beam, the velocity $\bar{v}$ is calculate to be 35.7m/sec.

$$\frac{1}{2}P\delta=\frac{P}{2}\frac{Pl^3}{3EI}=\frac{1}{2}m\bar{v}^2 \tag{9}$$

From Eq. (8), the damping coefficient C_f is given to be 9632kg/sec.

Total damping force is considered as a parallel connected dashpot model and C_{total} is obtained:

$$C_{total}=C+C_f=10318\text{kg/sec} \tag{10}$$

Finally, the damping ratio ζ is found as

$$\zeta=\frac{C_{total}}{2m\omega_n}=0.3 \tag{11}$$

The value of mass, 347kg, is a very conservative value since it approximately corresponds to that of steel and this value is obtained by assuming the outside and inside diameters of the insulation. If the line density of the composite pipe, 28.32kg/m, is used, the damping force is increased further. The stiffness of the broken pipe is obtained by assuming the system is a single degree of freedom. The stiffness is calculated to be $K=m\omega_n^2=18.39$kN/m where the first mode of the broken loop, 1.946Hz is used. If 39.4kN thrust force is applied at the broken node 60, the displacement is given by $\delta_1=F_1/K=2.14$m. If a steady state thrust force, 24.4kN is applied at the same node, $\delta_2=F_2/K=1.33$m. The initial velocity for both cases is obtained from $F\delta/2=mv^2/2$. The initial velocities for the applied force 39.4kN and 24.4kN, are given as 26.3m/sec and 16.2m/sec, respectively. The fluid damping caused by these applied forces is given by C_{f1}=5450kg/sec and C_{f2}=3590kg/sec, respectively. Taking the mean value of C_{f1} and C_{f2}, the equivalent damping factor is given

Table 3 Rayleigh damping coefficients

case no.	frequency range (Hz)	α	β	ζ
1	1.946~30	36.191	1.571×10^{-2}	1.576
2	6.3~30	19.63	2.63×10^{-3}	0.3
3	1.946~30	6.9512	2.987×10^{-3}	0.3
4	—	0	0	0

by C_f=4690kg/sec. The damping factor in the air is given by C=60.2kg/sec. The total damping ratio is obtained as $\zeta=(C_f+C)/2m\omega_n=1.576$.

The Rayleigh damping values are obtained for four cases, 1) broken loop, m=123kg, frequency range, 1.946Hz~30Hz, ζ=1.576, l=4.358m, 2) unbroken loop, m=347kg, frequency range, 6.3Hz~30Hz, ζ=0.3, l=5.334m, 3) m=347kg, frequency range, 1.946Hz~30Hz, ζ=0.3, l=5.334m, 4) no damping, ζ=0.0. The values of α and β in Rayleigh damping $2\zeta\omega=\alpha+\beta w^2$ for these cases are given in Table 3.

3.4 The dynamic responses for the preliminary study

The dynamic responses of the preliminary model is studied as a verification purpose. The dynamic responses are obtained using preliminary dynamic model with the boundary conditions shown in Fig. 2, and applied force history as given in Fig. 3.

The displacement responses at the broken section node 60 for the four cases are shown in Figs. 4 to 7. The maximum displacement is approximately 96.5cm in the z direction, since node 90 and 170 are not restrained in the z direction. This can be justified using the single freedom model. The stiffness of the broken pipe is $K=m\omega_n^2=18.39$kN/m. The steady state force at node 60 is 24.4kN as in Fig. 3. The displacement corresponding to the first mode is δ=1.33m. The displacement corresponding to the second mode of broken loop, f=2.2Hz, can be found as K=23.64kN/m and δ=1.032m. The value of 1.032m agrees reasonably with 96.5cm in Figs. 4 to 6. The displacement for ζ=0 is given as approximately 2.032m in Fig. 7. This can be the justified assuming the

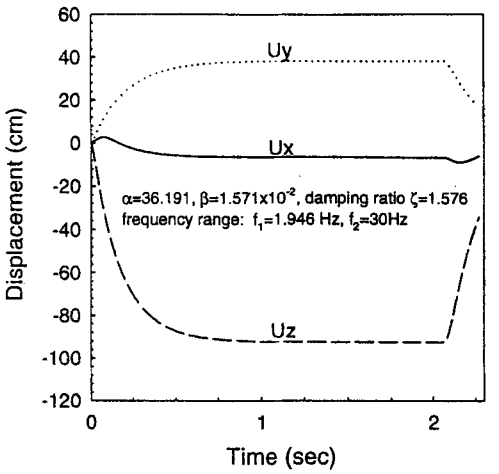

Fig. 4 Response at broken section (node 60) Preliminary dynamic model

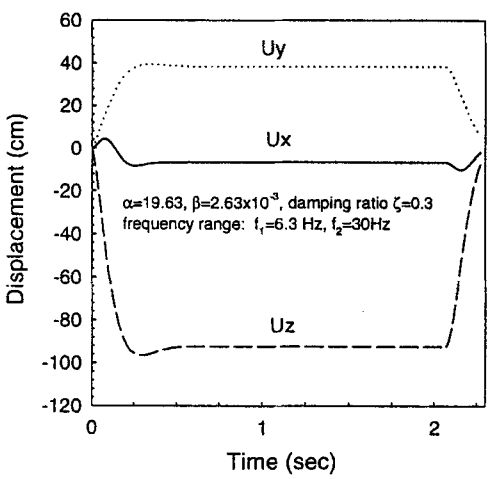

Fig. 5 Response at broken section (node 60) Preliminary dynamic model

single degree freedom system. If the applied force is a step function with magnitude 24.4kN in Fig. 3, the displacement of the spring-dashpot system is given by

$$x=\frac{F_0}{K}\left[1-\frac{e^{-\zeta\omega_n t}}{\sqrt{1-\zeta^2}}\cos(\omega_n t-\phi)\right] \quad (12)$$

where $\tan\phi=\zeta/\sqrt{1-\zeta^2}$, $\omega_d=\sqrt{1-\zeta^2}\omega_n$ (Thomson, 1965).

If ζ=0, $x=F_0(1-\cos\omega_n t)/K$, the maximum displacement x_{max} is calculated to be $x_{max}=2F_0/K$=2.083m. The value of 2.083m is reasonably close to 2.032m in Fig. 7. Also, the frequency

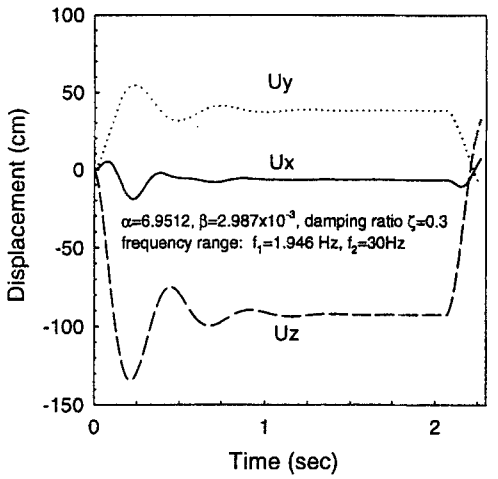

Fig. 6 Response at broken section (node 60) Preliminary dynamic model

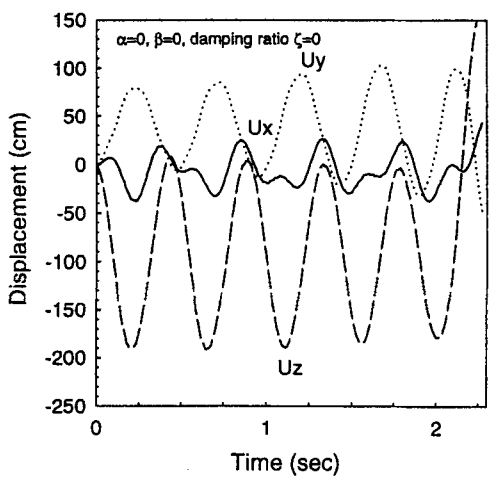

Fig. 7 Response at broken section (node 60) Preliminary dynamic model

appearing in Fig. 7 is approximately 2Hz, corresponding to the first and the second mode (f_1=1.946Hz and f_2=2.2Hz). The effective stress history is given as Fig 8. The effective stress is given as approximately 234kN/cm² at node 120. If the broken loop is considered as a cantilever beam fixed at node 120 and free at the broken section node 60, the displacement at the broken section node 60 is given by

$$\delta=\frac{Pl^3}{3EI},\ \frac{Pl}{I}=\frac{3E\delta}{l^2} \tag{13}$$

where δ=1.041m for the second mode. Then the

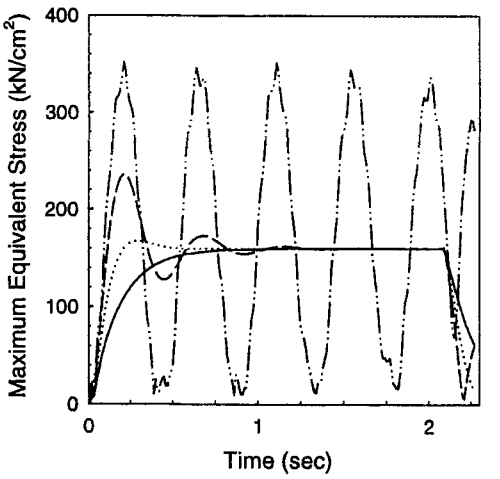

Fig. 8 Stress response at fixed node 120 (broken section 60) Preliminary dynamic model

bending stress is $\sigma=Plr_0/I$=219kN/cm². Similarly, the bending stress for the first mode is found to be 280kN/cm². If mean value is compared with the computer result, 234kN/cm², it may be considered as a reasonable value. Based on the comparison of the results obtained by rough hand calculation using the single degree freedom system with that of the computer results, it is concluded that the model is reasonable.

However, displacement responses at the broken sections are found to be so large that the ruptured pipe may collide with other structures with too high impact energy, which may result in failure of others. Therefore, the additional nodes, 186 and 112, are selected to be fixed in x-z directions and y-z directions, respectively, in final the model, while the model of the preliminary study does not include these constraints.

4. The Dynamic Responses of the Final Dynamic Model

The final dynamic model of the study, is slightly different from the preliminary dynamic model as mentioned above. In the model in section 3, nodes 120, 210 and 10 are fixed in the three directions, while nodes 90 and 170 are restrained in the y and x directions, respectively, and those points are not restrained in the z direction. The final model has more restraints, in addition to the

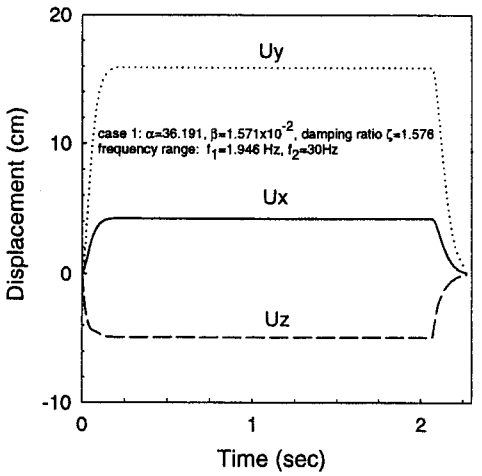

Fig. 9 Response at broken section (node 60) Final dynamic model

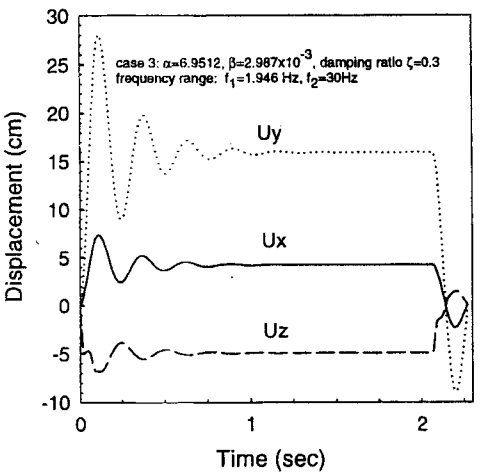

Fig. 11 Response at broken section (node 60) Final dynamic model

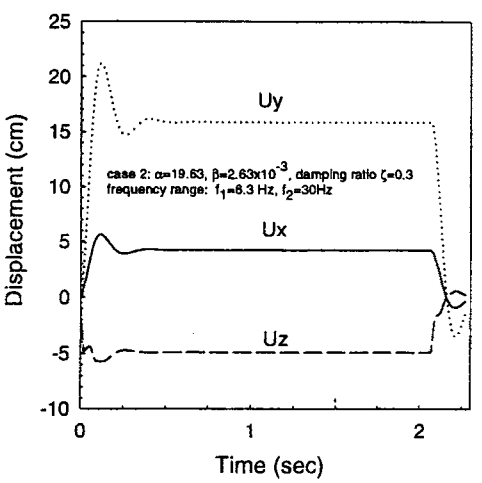

Fig. 10 Response at broken section (node 60) Final dynamic model

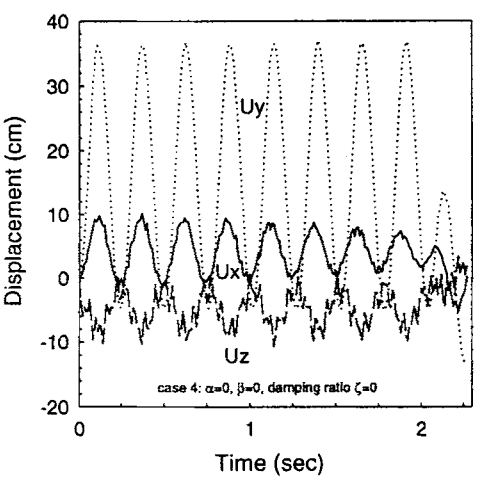

Fig. 12 Response at broken section (node 60) Final dynamic model

restraints of the preliminary model. Node 186 has the restraints in the x and z directions, and node 112 is constrained in the y and z directions in the final model.

The thrust force history given in Fig. 3 is applied independently at every postulated rupture section, nodes 60, 140, 110, 111, 200 and 201 in Fig. 2. The Rayleigh damping values α and β, obtained in the section 3, are used for four cases in the final model.

The displacements and velocities responses at the each broken section are found. Also the effective stresses at each fixed node, caused by each broken section, are found. The typical displacement response at the broken section, node 60, are given in Figs. 9 to 12. The effective stress responses at the fixed node 112, caused by the broken section, node 60, are given in Fig. 13. The dynamic responses at six broken sections and the effective stress responses at the fixed nodes, caused by each six broken sections, are summarized in Table 4.

5. Structural Integrity Evaluation

The dynamic responses at fixed nodes caused

Table 4 The dynamic responses at fixed and broken nodes (final dynamic model)

Broken node	Fixed node	Effective stress (kN/cm²)		Velocity at broken node (cm/sec)	Displacement (cm)
		Max.	Mean		
60	112 90	48 76	31 52	Max 381	Max 28
140	186 170	97 138	69 86	Max 509	Max 51
110	90	138	86	Mean 51	Mean 25
111	90	145	107	Mean 660	Mean 46
200	170	22	17	Mean 76	Mean 3.8
201	170	23	14	Mean 127	Mean 15

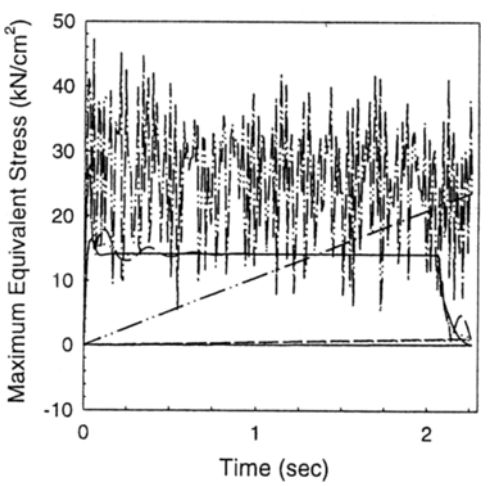

Fig. 13 Stress response at fixed node 112 (broken section 60) Final dynamic model

by each broken section are summarized in Table 4 and the straight distances between the fixed node and the broken node are summarized in Table 5. The mean value of the effective stress denotes the mean value of the stress of $\zeta=1.576$ and $\zeta=0$. From Table 4, the effective stress at each fixed node exceeds yielding stress 12.4kN/cm²(343℃) and the ultimate strength, $\sigma_u=42.5$kN/cm² of SA304-376, except nodes 112 and 170.

When the node 60 is broken, the thrust force will be in the direction of z. However, the force in the x and y direction is assumed to be half of mean thrust force $P=16$kN. The work done by thrust force, $U_1=P\delta/2=2.23$kJ, where $\delta=28$cm

Table 5 The straight distance between fixed and broken nodes, mass (final dynamic model)

Fixed mode	Node	Broken node	l(cm)	m(kg)
170	175	200 201	117	33
90	105	110 111	124	35
90	76	60	211	60
170	165	140	226	65

is the displacement at node 60 as shown in Table 4. The applied energy due to the bending moment at node 90 is $U_2=2.73$kJ. The total applied energy is $U_t=U_1+U_2=4.96$kJ and can be absorbed by the material within 5cm, since the toughness of the pipe per unit length is 1.33kJ/cm. Therefore, fixed node 90 cannot be broken. If the node 140 is broken, the stress at the fixed node 170 is given as 138kN/cm² and $\delta=51$cm in Table 4. The applied energy due to the thrust force is $U_1=4.07$kJ. The applied energy due to the bending moment is $U_2=9.04$kJ. The total applied energy is $U_t=U_1+U_2=13.11$kJ. This energy can be absorbed within the pipe length 10cm. Therefore, node 170 can not be broken. Furthermore, the fixed points are not fixed exactly and partial energy can be released at the points. Therefore, even though the stress at the fixed points exceeds the ultimate strength, a double ended guillotine

can not be expected.

6. The Structural Integrity of the Chimney Caused by the Pipe Whip

The chimney is a hexagonal structure surrounding the FTL in the pool. A ruptured loop at a given broken section in the FTL loop, can strike the chimney. Therefore, the integrity of the chimney caused by a broken pipe whip is evaluated.

The direction of the thrust of the broken sections at nodes 60 and 140 are both in the z direction. However, nodes 186 and 112 are fixed in the z direction and the motion in the z direction of the broken loop is small. In order to obtain conservative estimation, half of the mean thrust force is applied at nodes 60 and 140. The mean thrust force is applied at the nodes 200, 201, 110 and 111. Though the calculated mass of the broken loops is less than 175kg, it is conservatively considered to be 175kg for simplicity.

The thrust force applied at nodes 200, 201, 110, and 111 is 32kN. The chimney is made of SB209-type 6061-T6 aluminum alloy. Ultimate strength, $\sigma_u=26.2\text{kN/cm}^2$, yield strength, $\sigma_y=22.1\text{kN/cm}^2$, Young's modulus, $E=7.31\times10^6\text{N/cm}^2$, and density, $\rho=2.69\times10^{-3}\text{kg/cm}^3$. These values are obtained from the ASME-section Ⅲ material table, which is the minimum value. The thickness, width and height of the chimney are $t=2.54$cm, $l=40$cm and $h=335$cm, respectively. Six pieces of plate are welded in the direction of the height in a hexagonal shape. In order to simplify the calculation, the plate fixed two edges in the height direction is replaced by two edge fixed beam since the plate fixed two edges is stiffer than fixed-fixed beam.

The pipe whip energy is obtained from the study of the state of the design for pipe whip-NT-1320-Research Project-1334-2 Final Report. The thrust force applied at the broken sections, four nodes 200, 201, 110 and 111 in Fig. 2, is conservatively obtained to be 64.1kN. The thrust force at the broken sections, nodes 60 and 140, is obtained as 32kN.

The plastic moment caused by the plastic hinge at the fixed point is rotated as M_p. The moment, M_D, at the fixed point is caused by the drag force, F_D. Then the pipe whip energy, E, is found to be

$$E=(Tl-M_p-M_D)\theta$$
$$=\frac{1}{2}I_{rot}\omega^2=I_{rot}\left(\frac{v}{l}\right)^2 \tag{14}$$

where I_{rot}, θ and l are rotational moment of inertia at the fixed point, angle of rotation and maximum distance between broken section and the chimney, respectively. The initial velocity of the pipe, v, is obtained to be 2.04m/sec from Eq. (14).

Similarly, the velocity of the broken section at nodes 60 and 140 is obtained to be 12.9m/sec. The dynamic deflection is obtained by equivalent static loading given in J. Marin, Mechanical behavior of engineering materials, 1962.

$$y=y_s\left[1+\left(\frac{2h}{(1+w_e/w)\,y_s}\right)^{1/2}\right] \tag{15}$$

where y_s and w_e are static deflection caused by the dead weight applied at center of the beam and equivalent beam weight, respectively. For the dynamic deflection, y, it is assumed that the deflection caused by the ruptured pipe weight is applied by an impact on the center of the chimney from the height h in the gravity field. This is a very conservative assumption and h is found from the equation $v=\sqrt{2gh}$, when v is known. The dynamic deflection for large h is found approximately

$$y=\left[\frac{y_s v^2}{(1+\frac{w_e}{w})\,g}\right]^{1/2} \tag{16}$$

where $w_e\sim w_b$ (beam weight, 916N) and w (pipe weight, 636N). Hence, the plastic moment of the beam is $M_{ult}=1.2\times10^5$N-m. This value is greater than the bending moment at the fixed end $M=1\times10^5$N-m. Therefore, the integrity of the chimney would not be impeded due to a ruptured pipe whip.

The material toughness of the chimney made from aluminum alloy, $U_f=21.7\text{kN/cm}^2$. Volume of a piece of the chimney, $V=34900\text{cm}^3$. The total toughness of the beam, $U_t=U_fV=7.57\times10^6$J. This value is compared with ruptured pipe

whip energy. The pipe whip energy, E, given in Eq. (14) for the broken section nodes 60 and 140, is conservatively found to be 5.32×10^4J by neglecting the energy due to the drag force, which is much smaller than the material toughness. Therefore, the chimney is safe.

The next step is to evaluate the integrity using the results of the dynamic response obtained from the dynamic model and the computer.

The dynamic deflection, y, is found using Eq. (16). Eq. (16) is conservatively further simplified,

$$y\sim\left(\frac{y_s v^2}{2g}\right)^{1/2} \tag{17}$$

The dynamic deflection of Eq. (17) is obtained to be 1.27mm. The bending stress, $\sigma=Mc/I=1.6\times10^4$N/cm^2 which is less than $\sigma_y=22\times10^4$N/cm^2. Therefore, the chimney is safe. The other calculation is performed using the single degree freedom mass system. The dynamic deflection, y, is found as 0.2941cm, bending moment $M=1.326\times10^5$N-m. However, the plastic moment of the rectangular cross section is $M_{ult}=1.2\times10^5$N-m without including the strain hardening effect, which is reasonably close to the bending moment. The velocity of the mass obtained from the single degree freedom system is very conservative compared with that obtained by the computer (6.6m/sec). If the energy obtained by the single mass system is compared with the material toughness, the margin will increase further.

Through the various approximate engineering analyses and the results obtained by the computer, the integrity of the chimney under the condition of FTL loop rupture would not be impeded.

7. Conclusions

The static and seismic analysis using a static model of the fuel test loop(FTL), Korean multipurpose research reactor(KMRR), is performed and the results are compared with the results obtained by Battelle Northwest Research Institution. Dynamic analysis under the condition of a postulated FTL loop rupture is performed.

Six postulated rupture sections are assumed at the pipe connections in the FTL and these locations are chosen since static analysis shows that all the sections satisfy NUREG-0800 condition. The structural integrity evaluation of the chimney surrounding the FTL with a hexagonal shape made from welding six pieces of plate, is performed for the postulated FTL ruptures. Through computer analysis and approximate engineering calculations, the following results are found:

1) The results obtained by the static model are compared with the results obtained by the Battelle Research Institution. The results are compatible with Battelle's results. Therefore, static analysis can be justified.

2) The dynamic responses of the preliminary model is studied as a verification purpose. The results of analysis obtained using the preliminary dynamic model can be justified through rough engineering calculation. However, the dynamic response shows too large displacement at the broken sections. In the final dynamic model, nodes, 186 and 112, are chosen to be fixed as additional constraints.

3) Through the final dynamic model it is found that all the fixed points can be plastic hinged, while double ended guillotine can not be expected.

4) The structural integrity of the chimney under the conditions of FTL pipe rupture would not be impeded by the pipe whip.

References

Chang, Y. S., Seok, C. S. and Kim, Y. J., 1997, "Prediction of Fracture Resistance Curves for Nuclear Piping Materials (Ⅱ)," *KSME*, Vol. 21, No. 11, pp. 1786~1795.(in Korea)

Chang, Y. S., Seok, C. S. and Kim, Y. J., 1997, "Prediction of Fracture Resistance Curves for Nuclear Piping Materials (Ⅲ)-Development of computer Program for Fracture Resistance Curve Prediction," *KSME*, Vol. 21, No. 11, pp. 1796~1808.(in Korea)

Design Basis for Protection of Light Water Nuclear Power Plants Against the Effects of Postulated Pipe Rupture, *ANSI/ANS-58.2*,

1988.

Kwon, J. D., Moon, Y. B., and Kim, S. T., 1998, "A Study on the Application of Electrochemical Method for Degradation Evaluation," 1998, *KSME*, Vol. 22, No. 1, pp. 44~51.(in Korea)

Marin J., 1962, "Mechanical Behavior of Engineering Materials," *Prentice Hall*, N. J.

Postulated Pipe Rupture; Evaluation of Thrust Forces and Jet Impingement, Including Validity of Utilization of the Leak Before Break, *Battelle Northwest Research Institution*, 1995.

Song, S. H and Jhung, M. J., 1999, "Experimental Modal Analysis on the Core Support Barrel of Reactor Internals Using a Scale Model," *KSME International Journal*, Vol. 13, No. 8, pp. 585~594.(in Korea)

Study of the State of the Design for Pipe Whip, Nt-1320-Research Project-1334-2 Final Report, *Tennessee Valley Authority-Div. of Eng. Design*, 1980.

Thompson, W. T., 1965, "Vibration Theory Analysis and Application," *Prentice Hall*, N. J.

Timoshenko, S., 1955, "Strength of Materials, Vol Ⅰ," 1955, *D. Van Nostrand Co.*, N. J.